Journal of Pharmaceutical and Biomedical Analysis 56 (2011) 38–44

Contents lists available at ScienceDirect

Journal of Pharmaceutical and Biomedical Analysis

journal homepage: www.elsevier.com/locate/jpba

Characterization of drug–cyclodextrin formulations using Raman mapping and multivariate curve resolution

Balázs Vajna[a,*], István Farkas[a], Attila Farkas[a], Hajnalka Pataki[a], Zsombor Nagy[a], János Madarász[b], György Marosi[a]

[a] Department of Organic Chemistry and Technology, Budapest University of Technology and Economics, Budafoki út 8, H-1111 Budapest, Hungary
[b] Department of Inorganic and Analytical Chemistry, Budapest University of Technology and Economics, Szent Gellért tér 4, H-1111 Budapest, Hungary

ARTICLE INFO

Article history:
Received 25 February 2011
Received in revised form 20 April 2011
Accepted 6 May 2011
Available online 12 May 2011

Keywords:
Micro-Raman
Hyperspectral imaging
Chemometrics
Pharmaceutical
Cyclodextrin
Crystallinity

ABSTRACT

Raman chemical imaging was used in the characterization of drug–excipient interactions between a drug and different types of cyclodextrins. Detailed analysis was carried out regarding the interactions between the active ingredient (API) and the cyclodextrins and the heterogeneity of the samples was studied using multivariate curve resolution–alternating least squares algorithm. The amount of recrystallized pure API was also estimated using the same curve resolution method. The Raman mapping results were validated via scanning electron microscopy–energy dispersive X-ray spectroscopy and X-ray powder diffraction. Raman mapping was found to be suitable to detect traces of pure crystalline API below the detection limit of X-ray powder diffraction.

1. Introduction

The physical morphology, especially the amorphous state of drugs has gained great interest in the pharmaceutical technology. There are several advantages to the amorphous state, the most important of which is the increased dissolution rate due to higher molecular mobility. Since the water solubility of the majority of the recently synthesised and biologically effective molecules is very poor, the techniques to prepare the active ingredients in amorphous form are rapidly developing [1–3]. Increasingly popular methods are the preparation of solid dispersions via melt extrusion [4,5], electrospinning [6] and the formation of inclusion complexes with cyclodextrins [7,8].

The most remarkable challenge is usually the stabilization of the amorphous state. Chemical [9] as well as physical [9–11] stability issues may arise. While chemical stability is usually monitored using high performance liquid chromatography (HPLC) [12], multiple methods are used simultaneously to detect crystalline impurities [13,14], including differential scanning calorimetry (DSC), X-ray powder diffraction (XRPD), vibrational spectroscopy and solid state nuclear magnetic resonance (SSNMR) spectroscopy.

Chemical imaging, which is a currently emerging group of analytical methods combining vibrational spectrometry with microscopic imaging optics, has been also used for the analysis of amorphous drugs in solid dispersions. Mostly the distribution of the active ingredient is monitored, since its homogeneity influences the shelf life of the product [10,11]. However, not only the spatial distribution can be assessed, but the solid state characteristics can also be determined on the different domains on the measured surface, as there is a separate vibrational spectrum corresponding to each pixel of the investigated area [10].

The majority of studies evaluate the Raman and near-infrared chemical images in a univariate manner [4,5,10–12], although a large variety of multivariate methods have been applied in both chemical imaging [15–20] and spectroscopic characterization of crystallinity [14,21,22]. Connecting the two approaches, i.e. multivariate evaluation of vibrational chemical images is very promising in the detection and quantification of trace crystalline components in an amorphous system. Up to date, there is only one study dealing with this issue: Widjaja et al. investigated several drug-polymer solid dispersions and applied two factor analysis based algorithms: target transformation factor analysis and band-target entropy minimization [23]. However, no study is present in the literature where the most effective [24–26] curve resolution method, multivariate curve resolution–alternating least squares [27] is tested in the detection and characterization of trace crystallinity.

* Corresponding author. Tel.: +36 1463 5918.
E-mail address: balazs.vajna@gmail.com (B. Vajna).

0731-7085/$ – see front matter © 2011 Elsevier B.V. All rights reserved.
doi:10.1016/j.jpba.2011.05.005

Cyclodextrins are widely used to improve the dissolution characteristics of drugs [7] and can also help to stabilize the active ingredient in amorphous form [8]. In the present study, various types of cyclodextrins (alpha (ACD), beta (BCD), gamma (GCD), hydroxypropyl-beta (HPBCD), hydroxypropyl-gamma (HPGCD) and randomly methylated beta (RAMEB)) were used to form inclusion complex with a halogen-containing investigational drug in hydrochloride salt form. Raman mapping was combined with chemometric evaluation for three reasons: (1) to determine whether the inclusion complex was formed between the different types of cyclodextrins and the active ingredient, (2) to determine the spatial distribution of the ingredients and their physical morphology, (3) to detect and quantify the amount of residual trace crystallinity and non-complexed active ingredient. It was assumed that all these questions can be answered at the same time via proper evaluation of the Raman chemical images. In order to verify the Raman mapping results scanning electron microscopy combined with energy-dispersive X-ray spectroscopy (SEM–EDX, regarding the heterogeneity of samples) and X-ray powder diffraction (XRPD, regarding the degree of amorphization) were used.

2. Materials and methods

2.1. Materials and sample preparation

The hydrochloride salt of a commercially available drug with very poor water solubility was chosen as a model. Due to reasons of Industrial Property Rights (IPR) the drug is referred to as "API". Six types of cyclodextrins (ACD, BCD, GCD, HPBCD, HPGCD, RAMEB) were obtained from Wacker Chemie (Munich, Germany). The formulations of the API and cyclodextrins at 1:1 molar ratio were prepared with lyophilization method based on the technologies described in Refs. [28,29]. The active ingredient was dissolved in ethanol and was added to the cyclodextrin solution in water. The mixture was stirred for 30 min in each case. Ethanol was removed using a Labrota 4000 rotary evaporator (Heidolph Instruments, Schwabach, Germany) at room temperature and 10 mbar pressure. After removing the ethanol, the samples were lyophilized in a Lyovac GT-3 freeze dryer (Leybold AG, Hanau, Germany) for 10 h at 0.1 mbar pressure and −50 °C temperature. A secondary drying cycle was applied on each sample at 22 °C tray temperature for the duration of 5 h at 0.05 mbar pressure. All pure components were lyophilized as well before the measurements. All samples were ground after lyophilization.

2.2. X-ray powder diffraction (XRPD)

Samples were investigated in powder form. XRD patterns were obtained by a PANalytical X'pert Pro MPD X-ray diffractometer (Almelo, the Netherlands) equipped with an X'Celerator detector with 0.04 sollers, using Cu K_α radiation (1.542 Å) and Ni filter. The applied voltage was 40 kV while the current was 30 mA. The samples were analyzed between 2° and 42° 2θ. Automatic divergence and antiscatter slits were used to provide 10 mm irradiated length. Continuous scan was carried out with 0.0167° step size and 30.4 s counting time (overall measurement time was 10 min/sample). Five separate portions were scanned and their diffractograms were averaged for each sample.

2.3. Scanning electron microscopy–energy-dispersive X-ray spectroscopy (SEM–EDX)

Morphology of the samples was investigated by a JEOL 6380LVa (JEOL, Tokyo, Japan) type scanning electron microscope and elemental mapping was accomplished using the energy dispersive X-ray detector of the same equipment. Each specimen was fixed by conductive double sided carbon adhesive tape. The applied accelerating voltage was 15 kV, the working distance was 10 mm and during the elemental mapping the intensity of the detected X-ray radiation was between 5000 and 12,000 counts/s.

The heterogeneity of the active ingredient was assessed based on the distribution of chlorine atom, as it was used in hydrochloride salt form. The oxygen atom is only present in the cyclodextrins and not the API, thus, its distribution was used to determine the heterogeneity of the excipient.

2.4. Raman chemical imaging

Raman mapping spectra were collected using a Horiba Jobin-Yvon LabRAM system coupled with an external 532 nm frequency-doubled Nd-YAG laser source and an Olympus BX-40 optical microscope. An objective of 10× magnification was used for optical imaging and spectrum acquisition. The instrument is described elsewhere [26]. All spectra were obtained in the spectral range of 290–1740 cm^{-1} with approximately 3 cm^{-1} resolution provided by a grating monochromator of 1800 groove/mm.

All samples were investigated in powder form. No further sample preparation was applied. Raman maps were collected with 10× objective (laser spot size: ~3 μm) and 40 μm step size. In each experiment the acquisition time of a single spectrum was 1 s and 5 spectra were averaged at each spatial position. The measured area varied from 0.8 mm × 0.8 mm to 1 mm × 1 mm.

The reference Raman spectra of the pure ingredients were collected with a 100× objective using sufficient acquisition times to achieve adequate signal-to-noise ratio (the actual measurement time depended on the materials themselves).

2.5. Data analysis of chemical images

Before chemometric evaluation, all spectra were base-line corrected (this was done by using the same baseline points for all the maps and reference spectra). The raw three-dimensional data was unfolded into a 2-dimensional matrix (for the procedure see Ref. [16]).

The estimation of pure component spectra (further also referred to as 'loadings') from the Raman maps was carried out by multivariate curve resolution–alternating least squares (MCR–ALS [27]). Applied constraints were non-negativity of concentrations, non-negativity of spectra and closure (the sum of scores was forced to be 1 at each pixel). All calculations were performed in MATLAB 7.6.0 (Mathworks, USA) with PLS_Toolbox 6.0.1 and MIA_Toolbox 2.0.1 (Eigenvector Research, USA).

Spectral concentrations of the ingredients present in the sample (further also referred to as 'Raman scores' in order to avoid confusion with real concentrations) were computed using MCR–ALS. The calculations are based on the following bilinear model:

$$\mathbf{X} = \mathbf{C}\mathbf{S}^{\mathrm{T}} + \mathbf{E} \quad (1)$$

$\mathbf{S}^{\mathrm{T}}$ ($k \times \lambda$) is the set of reference (pure component) spectra, $\mathbf{X}$ ($p \times \lambda$) is the matrix containing the mapping spectra, and $\mathbf{C}$ ($p \times k$) contains the vectors of spectral concentrations (each row in $\mathbf{C}$ contains the concentrations of the k ingredients). The matrix $\mathbf{E}$ represents the residual noise. The CLS calculation, which provides the $\mathbf{C}$ matrix using $\mathbf{X}$ and $\mathbf{S}^{\mathrm{T}}$, is described in numerous papers, including [15–19]. For the visualized score maps, scores were calculated with CLS method using the reference spectra of the pure ingredients.

Visualization of spectra and spectral concentration maps was carried out with LabSpec 5.41 (Horiba Jobin Yvon, France). The statistical properties of scores (mean, standard deviation) were computed with MATLAB.

3. Results and discussion

Formation of inclusion complexes with cyclodextrins can enhance the solubility of a drug to a large extent, but the long term stability is ensured only if the whole amount of the API interacts with the cyclodextrin. Raman mapping has proven to be a versatile method in the analysis of solid dispersions [4,5,10–12], thus, this method was used in this study to characterize the drug–excipient interactions. Six types of cyclodextrins were compared, using an efficient preparation method [28,29], to determine which one yields the most complete complexation. Raman mapping was performed on each sample and the vast amount of information present in the Raman maps were extracted first via conventional, then via chemometric approaches.

Conventional evaluation provides already a significant amount of valuable knowledge including the average spectrum of the chemical image, which gives a general idea about the bulk structure of the sample. Furthermore, the visualized score maps (as the Raman scores correspond to the concentrations) give insight into the spatial distribution of the ingredients and may reveal local deviations in an otherwise homogeneous environment (e.g. local crystallization of pure API can be detected with high sensitivity, while the majority of the API is present in the form of inclusion complex).

Using curve resolution algorithms, such as MCR–ALS, helps to discover, however, further details. The resolved pure component spectra with MCR–ALS show the underlying factors in the dataset (it has to be noted that "pure components" in the terms of curve resolution may not always be chemically pure, thus they are often referred to as 'loadings' to avoid miscomprehension). Finally, using the Raman scores calculated with MCR–ALS, estimation can be given to the ratio of amorphous and crystalline inclusion complexes and the pure active ingredient present in non-complex form.

3.1. Inspection of average spectra

The position of the vibrational bands in the average spectra of the chemical images indicates the general morphology of the system, giving the same type of information as if the samples were investigated with a conventional (non-imaging) vibrational spectroscopic method.

The spectral differences between the inclusion complex and crystalline form are shown in Fig. 1. The spectrum on the top is the reference spectra from the pure, crystalline API (spectrum 1a). Two peaks can be seen at 1581 and 1586 cm^{-1}; furthermore, a sharp peak appears at 1372 cm^{-1}. It is indicated by spectra 1b and 1c, that the API does not form inclusion complex with the alpha and beta cyclodextrins, as the properties of the API peak do not change. However, it cannot be proved based on the average spectra that the formation of inclusion complex does not take place locally in certain regions of the sample.

The changes of peak positions and shapes refer to structural changes. The most important change in the spectrum of API + GCD (spectrum 1d) lyophilized mixture is that the peak at 1586 cm^{-1} disappears, while the peak at 1581 cm^{-1} remains with a slight shift to 1580 cm^{-1}. Besides, significant, asymmetric band widening can be observed towards lower wavenumbers on the peak at 1372 cm^{-1}. This indicates that significant interaction exists between the ingredients, i.e. the GCD molecule is large enough to form inclusion complex with the active substance.

In the case of alkylated cyclodextrin derivatives (HPBCD, HPGCD, RAMEB; spectra 1e, 1f and 1g, respectively) higher degree of (and symmetric) widening can be observed on the API peaks. Furthermore, the maximum of the peak at originally 1372 cm^{-1} shifts to lower wavenumbers (1371–1368 cm^{-1}). Such band broadening indicates the occurrence of amorphization.

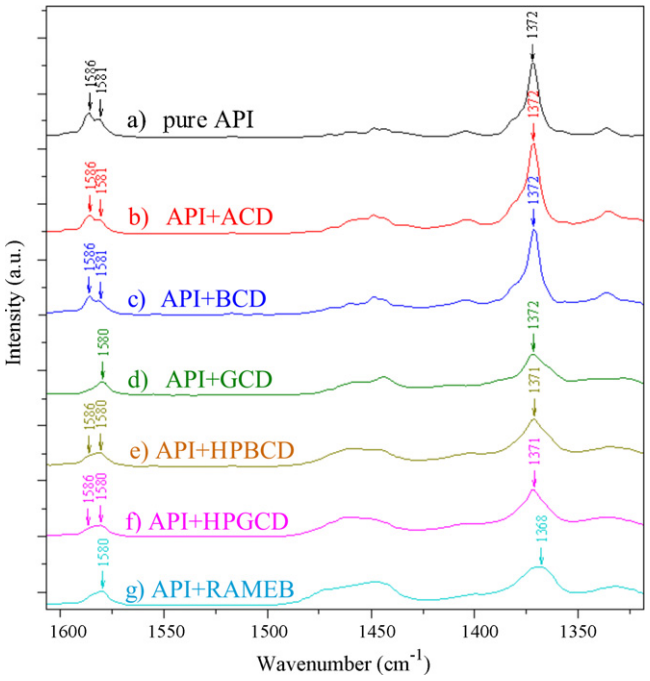

Fig. 1. Peaks of active ingredient in the average spectra of Raman maps (spectra were normalized to unit area for illustration).

3.2. Evaluation of chemical images

The visualized score images give insight into the spatial distribution and heterogeneity of the components. Fig. 2 shows the results obtained with the different analytical methods (Raman mapping, SEM–EDX imaging, XRPD).

Fig. 2a, d, g, j, m and p shows the distribution of the active ingredient. The Raman scores of the pure components were calculated with direct classical least squares method using the pure reference spectra of the API and the respective cyclodextrins. The Raman score (i.e. spectrally calculated concentration) of the API in each pixel is indicated by the colour scale on the right of each distribution map. In certain areas the vibrational peaks of the API uniformly emerged with fairly low intensities (thus, its calculated concentration was low), shown with blue on the Raman figures. The homogeneity in these areas suggests that the API forms complex with the cyclodextrin. However, the pure API has very intensive Raman signals; therefore, where peaks of the pure API are very prominently seen in the measured spectrum, pure API particles can be assumed to be present in the sampled volume. This phenomenon results in the fact that where pure API is also present, the calculated Raman CLS scores for the API are significantly higher than in the regions where it is present in complex form. Fig. 3 contains representative mapping spectra of differently coloured regions within the Raman maps.

It can be seen in Fig. 2a and d that the distribution of API is completely heterogeneous and is present as distinct particles in the ACD–API and BCD–API samples. Besides, Fig. 3a illustrates that the API is present in crystalline state, regardless of its observed concentration level in any pixel. The corresponding SEM–EDX images (Fig. 2b and e) support these observations, as the distinct particles either contain pure API (green) or pure cyclodextrin (red). Since the formation of inclusion complex would result in identical spatial distribution of the two components, these figures indicate that ACD and BCD do not form inclusion complex with the active ingredient. This is in correspondence with the X-ray diffractograms (Fig. 2c and f), which shows that the amorphization was not successful in these cases.

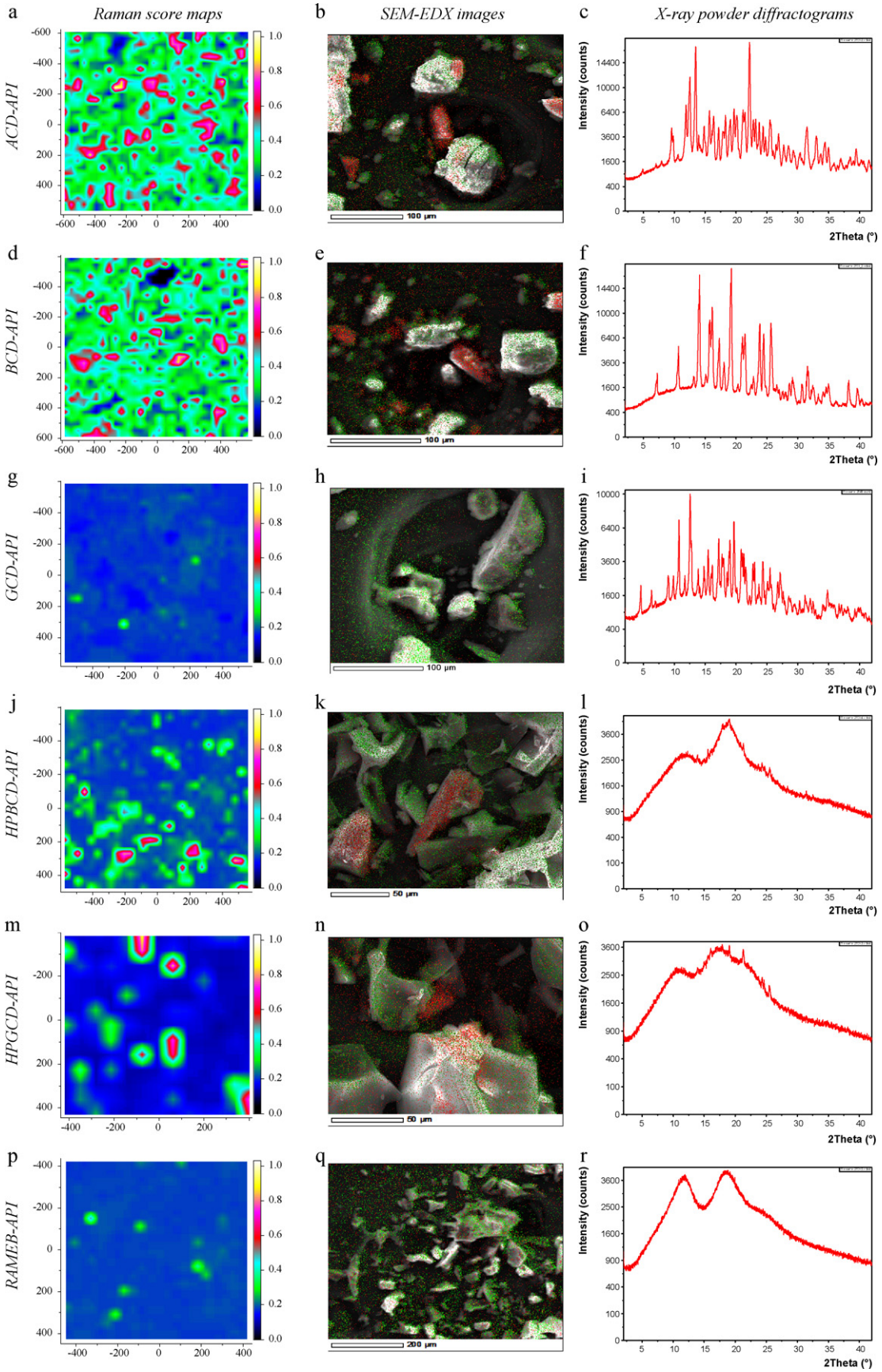

Fig. 2. Raman score maps, SEM–EDX images and X-ray powder diffractograms of the API–cyclodextrin lyophilized mixtures.

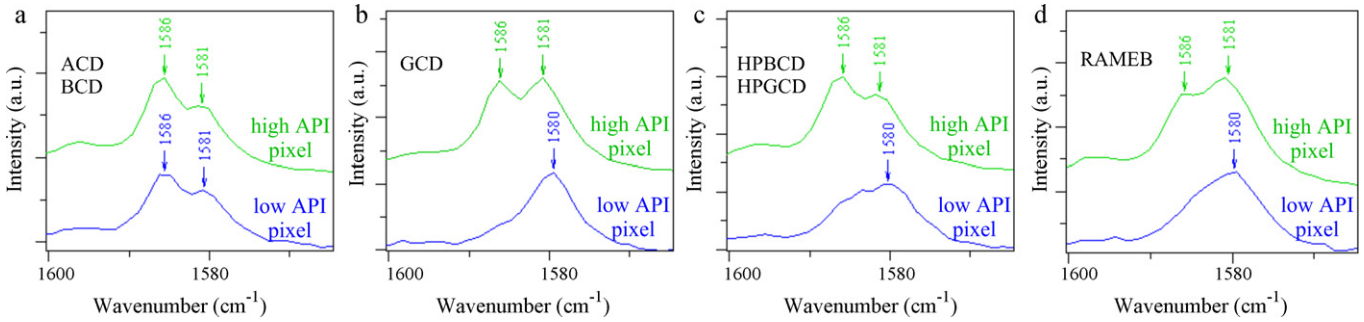

Fig. 3. Examples of mapping spectra from pixels with high and low observed API concentrations.

The results in the case of GCD–API sample are shown in Fig. 2g, h and i. The distribution of the API is generally homogeneous (except for a small number of pixels), indicating that GCD is capable of forming inclusion complex with the API (Fig. 2g). The SEM–EDX image (Fig. 2h) confirms that the two ingredients are not separated from each other, as both red (GCD) and green (API) points are uniformly distributed in the whole image. Fig. 3b (blue spectrum) shows that in those areas, where the API is homogeneously distributed, its peaks are altered implying interaction with the cyclodextrin. The fact that significant band broadening was not observed in the Raman mapping spectra is in correspondence with the X-ray diffractogram (Fig. 2i), which shows that the inclusion complex is not amorphous but crystalline. However, it has to be noted, that a few points on the Raman score image proves the presence of non-complexed active ingredient (coloured green in Fig. 2g and spectrum shown with green in Fig. 3b), while this could not be detected at all with any of the other methods.

According to Fig. 2j and m, the API is present in all the measured points of the HPBCD–API and HPGCD–API samples, showing that the complexation took place to some extent. The alteration of a characteristic API peak in the blue areas of Fig. 2j and m is shown in Fig. 3c. However, there are district particles containing API in high concentration as well. This is validated by the SEM–EDX images (Fig. 2k and n), on which API rich domains (green) can be observed. The X-ray powder diffractograms (Fig. 2l and o) confirm the assumptions based on the Raman results, i.e. the HPBCD–API and HPGCD–API complexes are in amorphous form (this is most likely due to the fact that the alkylated cyclodextrins themselves are amorphous in pure form). Although the amount of crystalline non-complexed API is only slightly above the XRPD limit of detection, the Raman score images significantly denote the presence of crystalline particles.

Fig. 2p shows that the distribution of API is almost completely homogeneous in the API–RAMEB formulation, except in a few distinct pixels. The SEM–EDX image (Fig. 2q) also shows proper dispersion of the two components. This means that the complexation took place between the RAMEB cyclodextrin and the API. The Raman image very sensitively shows the appearance of trace crystallinity, as in the majority of the corresponding pixels the crystalline peaks (1372 and 1586 cm^{-1}) only appear slightly or as a 'shoulder' near the peak at 1580 cm^{-1} (Fig. 3d). Fig. 2r proves that the small amount of crystalline API detected by Raman mapping is below the limit of detection of the conventionally used XRPD, even though the overall measurement time was approximately the same.

It can be concluded based on Fig. 2 that the complexation could take place in the cases of GCD and the alkylated cyclodextrins; however, despite the 1:1 molar ratio used, some of the active ingredient was detected in pure form. Either the complexation did not take place completely during the formulation, or the complex form is not thermodynamically stable and recrystallization occurs after the procedure.

3.3. Inspection of resolved spectra via MCR–ALS

The previous sections show that the average spectra (such as those obtained with a non-imaging spectrometer) and the distribution maps created with conventional evaluation methods already enable thorough characterization of the drug–excipient samples, revealing the interactions and giving a qualitative idea about the amount of residual non-complexed API present. However, further information can be gained if the above steps are followed by MCR–ALS decomposition.

All deductions in Sections 3.1 and 3.2 were made based on visual inspection of the spectral concentration maps and the individual mapping spectra. General statements, such as the relation between the observed API Raman score and the complexation (described in the beginning of Section 3.2) can only be drawn if they have been confirmed by inspecting every mapping spectrum. This is a very time-consuming procedure and still some features cannot be extracted this way, e.g. the spectrum of a trace substance which highly overlaps with the signals of other components. The advantage of chemometric curve resolution methods is that they utilize the entire spatial and spectral information of the dataset at the same time, providing more accurate results in relatively short time.

Multivariate curve resolution techniques, such as MCR–ALS, are capable of estimating the underlying factors in the dataset. Although this is also possible using factor analysis based algorithms [23], the advantage of MCR–ALS is that physically meaningful scores (concentrations) and loadings (spectra) are used throughout the calculations, rendering it particularly effective for spectral datasets [24–26].

MCR–ALS decomposition of the Raman maps yielded two loadings in all cases, meaning that the lyophilized mixtures consist of two components (it should be noted that MCR–ALS requires the number of components as input information, however, a trial and error approach assuming different numbers of pure components led to the conclusion that there are no more than two components present in each case). The first loading is equivalent to the Raman spectrum of the pure, crystalline active ingredient in all cases. Its resolution was successful even in the case of RAMEB cyclodextrin–API freeze dried product, where the crystalline peaks were the most overlapped by the bulk signal.

The second loading, however, is not identical among the different samples, indicating differences in the drug–cyclodextrin interaction. As shown in Fig. 4, the second loading corresponds to the pure cyclodextrin in the case of the ACD–API and BCD–API mixtures. In these two cases the cyclodextrin loadings do not contain any contribution from the active ingredient, meaning that the spectra of the API and these cyclodextrins are spatially completely independent and all measured Raman spectra in the chemical image are a mixture of the spectra of the two pure components. In contrast, the second loading contains both cyclodextrin and API peaks in the cases of GCD and the alkylated cyclodextrins (HPBCD, HPGCD and RAMEB). The most prominent API peak appearing on

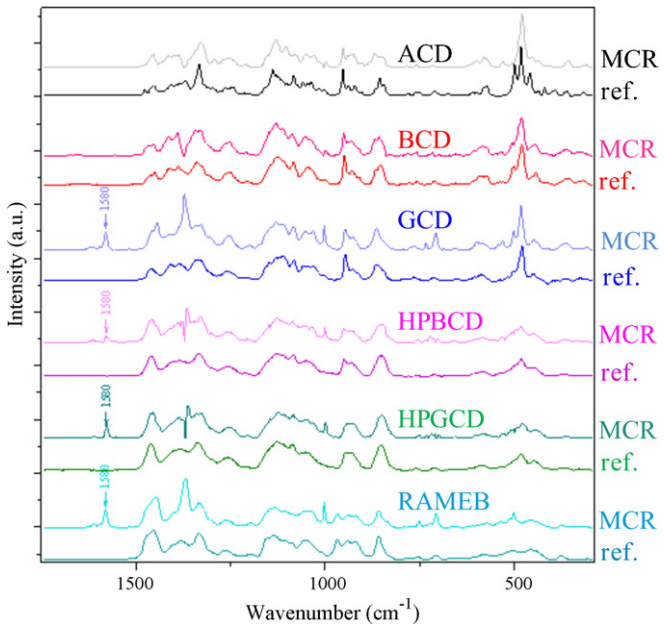

Fig. 4. MCR–ALS resolved spectra corresponding to the cyclodextrin obtained from the Raman maps of the different cyclodextrin–API lyophilized mixtures.

the loadings is marked by an arrow and its position (1580 cm^{-1}) is shown on the wavelength scale. Closer inspection reveals that these API peaks are different from the peaks of the pure crystalline API, and similar deviations can be seen as those described in Section 3.1 (e.g. the disappearance of the band at 1586 cm^{-1}).

It should be also noted that in some cases relatively 'negative' peaks were observed in the second loading. This may happen when both loadings have similarly high intensities at the same or nearby wavenumbers, i.e. they have an almost completely overlapping peak. At these wavenumbers the true intensity in the pure spectra cannot be determined and the true solution is ambiguous. Iterations in this case can result in a wide range of solutions. The degree of ambiguity, i.e. the feasible range of possible solutions can be calculated with advanced curve resolution methods [30,31] (they were, however, not applied here as this issue had no practical importance in this case. Since only the peak around 1370 cm^{-1} is significantly affected, the ambiguity in the calculated concentrations is negligible).

3.4. Estimation of the degree of crystallinity and amount of non-complexed API

The MCR–ALS calculations discussed in Section 3.3 also provided Raman scores both for the non-complexed API and the API–cyclodextrin inclusion complex. Plotting the MCR–ALS scores against the spatial coordinates makes it possible to make the statements drawn in Section 2 more clear and evident. Fig. 5 proves that all deviations from the otherwise homogeneous distribution of the active ingredient in the Raman maps in Fig. 2 were caused by the crystallization of the API (higher API scores in Fig. 2 appear at the same coordinates as where crystalline API is detected by MCR in Fig. 5). Furthermore, at areas where the API was detected with homogeneously low spectral concentrations in Fig. 2, no API in crystalline or non-complexed state was detected with MCR-ALS.

In addition, these scores, although not being equal to the real concentrations, can be used as rough estimation of the crystalline material present. The observed Raman scores for the non-complexed, crystalline API are the following: GCD–API: 1.33%; HPBCD–API: 4.0%; HPGCD–API: 4.5%; RAMEB–API: 0.9%. Percentage values were obtained by multiplying the MCR–ALS scores with 100% (as originally scores were scaled between 0 and 1). The obtained values are in good agreement with the X-ray diffractograms: while the crystalline API is already detected by XRPD in the HPBCD–API and HPGCD–API samples, the trace crystallinity in the RAMEB–API sample is below its limit of detection. This shows that Raman mapping can be a very useful tool in the detection of the early stages of crystallization. Besides, using an appropriate calibration set, better quantification can be expected with Raman mapping

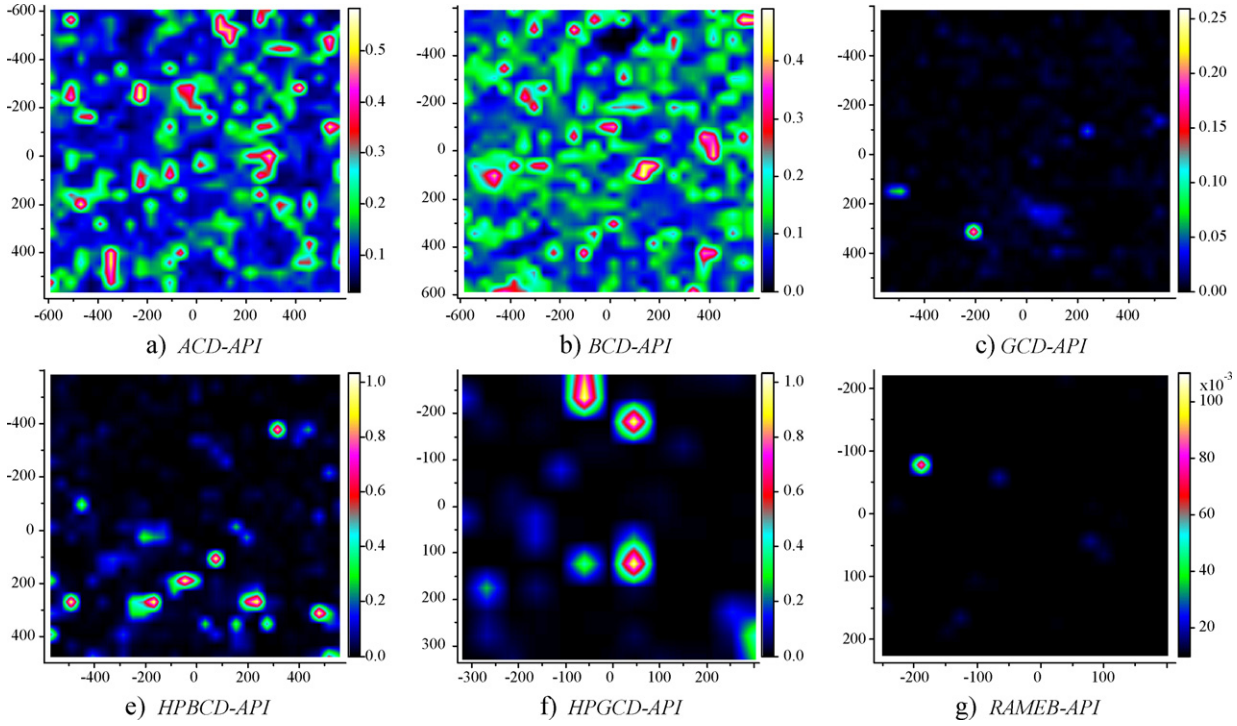

Fig. 5. Distribution of crystalline, non-complexed API in the API–cyclodextrin formulations, calculated with MCR–ALS.

at 3–5% crystalline content than with XRPD, as just above the limit of detection quantification is still inaccurate. As it is shown in Fig. 2j and m, this degree of crystallinity is well above the limit of detection of the Raman images with an appropriate size of measured area.

Additionally, it can be seen that using Raman mapping the complexation can be investigated successfully even when the resulting inclusion complex is not amorphous. The amount of remaining traces of non-complexed API could be estimated (1.33%) in the case of the GCD–API lyophilized mixture despite its very low concentration, while this cannot be carried out with XRPD as the diffractogram is dominated by the peaks of the inclusion complex.

4. Conclusions

It was demonstrated that the combined use of Raman chemical imaging and MCR–ALS evaluation method is rather effective in the detailed characterization of drug–excipient interactions. The average spectra and the loadings provided by MCR–ALS help determine whether there is interaction among the ingredients (in this case, whether the inclusion complex was formed). The high selectivity of Raman bands enable the estimation of the physical morphology and the amorphization can be monitored based on the alterations in the API Raman peak positions and shapes. The visualized score images give insight into the distribution of the ingredients revealing if any local deviation exist from the bulk characteristics. Traces of non-complexed API were unambiguously detected in both crystalline and amorphous inclusion complexes below the XRPD limit of detection. Additionally, semi-quantitative estimation was given for the amount of non-complexed crystalline API using the scores obtained with MCR-ALS.

This study shows that the combination of Raman chemical imaging and chemometric evaluation is a versatile tool, being able to answer several questions based on single set of measurements. This technique can play an important role in the characterization of drug–excipient interactions and amorphous materials.

Acknowledgements

The research was supported by the OTKA Research Fund (code K76346), ERA Chemistry (code NN 82426), W2Plastics EU7 Project (code 212782), and the Hungarian projects TECH_08-A4/2-2008-0142 and TAMOP-4.2.1/B-09/1/KMR-2010-0002.

References

[1] L. Yu, Amorphous pharmaceutical solids: preparation, characterization and stabilization, Adv. Drug Deliv. Rev. 48 (2001) 27–42.
[2] B.C. Hancock, G.J. Zografi, Characteristics and significance of the amorphous state in pharmaceutical systems, J. Pharm. Sci. 86 (1997) 1–12.
[3] G.G.Z. Zhang, D. Law, E.A. Schmitt, Y. Qiu, Phase transformation considerations during process development and manufacture of solid oral dosage forms, Adv. Drug Deliv. Rev. 56 (2004) 371–390.
[4] J. Breitenbach, W. Schrof, J. Neumann, Confocal Raman-spectroscopy: analytical approach to solid dispersions and mapping of drugs, Pharm. Res. 16 (1999) 1109–1113.
[5] E. Karavas, M. Georgarakis, A. Docoslis, D. Bikiaris, Combining SEM, TEM, and micro-Raman techniques to differentiate between the amorphous molecular level dispersions and nanodispersions of a poorly water-soluble drug within a polymer matrix, Int. J. Pharm. 340 (2007) 76–83.
[6] Zs.K. Nagy, K. Nyúl, I. Wágner, K. Molnár, Gy. Marosi, Electrospun water soluble polymer mat for ultrafast release of Donepezil HCl, Express Polym. Lett. 4 (2010) 763–772.
[7] K. Uekama, F. Hirayama, T. Irie, Cyclodextrin drug carrier systems, Chem. Rev. 98 (1998) 2045–2076.
[8] G. Patyi, A. Bódis, I. Antal, B. Vajna, Zs. Nagy, G. Marosi, Thermal and spectroscopic analysis of inclusion complex of spironolactone prepared by evaporation and hot melt methods, J. Therm. Anal. Calorim. 102 (2010) 349–355.
[9] J.F. Willart, M. Descamps, Solid state amorphization of pharmaceuticals, Mol. Pharm. 5 (2008) 905–920.
[10] A. Docoslis, K.L. Huszarik, G.Z. Papageorgiou, D. Bikiaris, A. Stergiou, E. Georgarakis, Characterization of the distribution, polymorphism, and stability of nimodipine in its solid dispersions in polyethylene glycol by micro-Raman spectroscopy and powder X-ray diffraction, AAPS J. 9 (2007) E361–E370.
[11] N Furuyama, S. Hasegawa, T. Hamaura, S. Yada, H. Nakagami, E. Yonemochi, K. Terada, Evaluation of solid dispersions on a molecular level by the Raman mapping technique, Int. J. Pharm. 361 (2008) 12–18.
[12] S. Šašić, A comparison of Raman chemical images produced by univariate and multivariate data processing – a simulation with an example from pharmaceutical practice, Analyst 129 (2004) 1001–1007.
[13] F. Zhang, J. Aaltonen, F. Tian, D.J. Saville, T. Rades, Influence of particle size and preparation methods on the physical and chemical stability of amorphous simvastatin, Eur. J. Pharm. Biopharm. 71 (2009) 64–70.
[14] G.A. Stephenson, R.A. Forbes, S.M. Reutzel-Edens, Characterization of the solid state: quantitative issues, Adv. Drug Deliv. Rev. 48 (2001) 67–90.
[15] A.A. Gowen, C.P. O'Donnell, P.J. Cullen, S.E.J. Bell, Recent applications of chemical imaging to pharmaceutical process monitoring and quality control, Eur. J. Pharm. Biopharm. 69 (2008) 10–22.
[16] C. Gendrin, Y. Roggo, C. Collet, Pharmaceutical applications of vibrational chemical imaging and chemometrics: a review, J. Pharm. Biomed. Anal. 48 (2008) 533–553.
[17] J.M. Amigo, Practical issues of hyperspectral imaging analysis of solid dosage forms, Anal. Bioanal. Chem. 398 (2010) 93–109.
[18] K.C. Gordon, C.M. McGoverin, Raman mapping of pharmaceuticals, Int. J. Pharm. doi:10.1016/j.ijpharm.2010.12.030.
[19] S. Šašić, An in-depth analysis of Raman and near-infrared chemical images of common pharmaceutical tablets, Appl. Spectrosc. 61 (2007) 239–250.
[20] B. Vajna, I. Farkas, A. Szabó, Z. Zsolt, G. Marosi, Raman microscopic evaluation of technology dependent structural differences in tablets containing imipramine model drug, J. Pharm. Biomed. Anal. 51 (2010) 30–38.
[21] A. Heinz, M. Savolainen, T. Rades, C.J. Strachan, Quantifying ternary mixtures of different solid-state forms of indomethacin by Raman and near-infrared spectroscopy, Eur. J. Pharm. Sci. 32 (2007) 182–192.
[22] J. Rantanen, H. Wikstroem, F.E. Rhea, L.S. Taylor, Improved understanding of factors contributing to quantification of anhydrate/hydrate powder mixtures, Appl. Spectrosc. 59 (2005) 942–951.
[23] E. Widjaja, P. Kanaujia, G. Lau, W.K. Ng, M. Garland, C. Saal, A. Hanefeld, M. Fischbach, M. Maio, R.B.H. Tan, Detection of trace crystallinity in an amorphous system using Raman microscopy and chemometric analysis, Eur. J. Pharm. Sci. 42 (2010) 45–54.
[24] L. Duponchel, W. Elmi-Rayaleh, C. Ruckebusch, J.P. Huvenne, Multivariate curve resolution methods in imaging spectroscopy: influence of extraction methods and instrumental perturbations, J. Chem. Inf. Model. 43 (2003) 2057–2067.
[25] C. Gendrin, Y. Roggo, C. Collet, Self-modelling curve resolution of near infrared imaging data, J. Near Infrared Spectrosc. 16 (2008) 151–157.
[26] B. Vajna, G. Patyi, Z. Nagy, A. Bódis, A. Farkas, G. Marosi, Comparison of chemometric methods in the analysis of pharmaceuticals with hyperspectral Raman imaging, J. Raman Spectrosc. (2011), doi:10.1002/jrs.2943.
[27] R. Tauler, Multivariate curve resolution applied to second order data, Chemom. Intell. Lab. Syst. 30 (1995) 133–146.
[28] J. Pitha, T. Hoshino, Effects of ethanol on formation of inclusion complexes of hydroxypropyl cyclodextrins with testosterone or with methyl orange, Int. J. Pharm. 80 (1992) 243–251.
[29] J. Pitha, T. Hoshino, J. Torres-Labandeira, T. Irie, Preparation of drug–hydroxypropyl cyclodextrin complexes by a method using ethanol or aqueous ammonium hydroxide as co-solubilizers Int, J. Pharm. 80 (1992) 253–258.
[30] R. Tauler, Calculation of maximum and minimum band boundaries of feasible solutions for species profiles obtained by multivariate curve resolution, J. Chemometr. 15 (2001) 627–646.
[31] R. Rajkó, Computation of the range (band boundaries) of feasible solutions and measure of the rotational ambiguity in self-modeling/multivariate curve resolution, Anal. Chim. Acta 645 (2009) 18–24.